Evapotranspiration and energy partitioning across a forest-shrub vegetation gradient in a subarctic, alpine catchment

Erin M. Nicholls[1], Sean K. Carey[1]

[1]School of Earth, Environment and Society, McMaster University, Hamilton, Ontario, Canada, L8S 4K1

Correspondence to: E.M. Nicholls (nicholem@mcmaster.ca)

Abstract

As a result of altitude and latitude amplified climate change, widespread changes in vegetation composition, density and distribution have been observed across northern regions. Despite wide documentation of shrub proliferation and treeline advance, few field-based studies have evaluated the hydrological implications of these changes. Quantification of total evapotranspiration (ET) across a range of vegetation gradients is essential for predicting water yield, yet challenging in cold alpine catchments due to heterogeneous land cover, including both boreal forest and shrub taiga ecosystems. Here, we present six years of surface energy balance components and ET dynamics at three sites along an elevational gradient in a subarctic, alpine catchment near Whitehorse, Yukon Territory, Canada. These sites span a gradient of thermal and vegetation regimes, providing a space-for-time comparison for future ecosystem shifts: 1) a low-elevation boreal white spruce forest (~12-20 m), 2) a mid-elevation subalpine taiga comprised of tall, dense willow (*Salix*) and birch (*Betula*) shrubs (~1-3 m) and 3) a high-elevation subalpine taiga with short, sparse shrub cover (< 0.75 m) and moss, lichen, and bare rock. Eddy covariance instrumentation ran year-round at the forest and during the growing season at the two shrub sites. Total ET decreased and interannual variability increased with elevation, with mean May to September ET totals of 349 (±3) mm at the forest, 249 (±10) mm at the tall, dense shrub site, and 240 (± 26) mm at the short, sparse shrub site. Comparatively, over the same period, ET:R ratios were the highest and most variable at the forest (2.19 ± 0.37) and similar at the tall, dense shrub (1.22 ± 0.09) and short, sparse shrub (1.14 ± 0.05) sites. Our results suggest that advances in treeline will increase overall ET and lower interannual variability; however, the large growing season water deficit at the forest indicates strong reliance on soil moisture from late fall and snowmelt recharge. In contrast, ET was considerably less at the cooler higher elevation shrub sites, which exhibited similar ET losses over 6 years despite differences in shrub height and abundance. ET rates between the two shrub sites were similar throughout the year, except during the peak growing season. Greater interannual variability in ET at the short, sparse shrub site indicates the reduced influence of vegetation controls on ET. Results suggest that predicted changes in vegetation type and structure in northern regions will have a considerable impact on water partitioning and will vary in a complex way in response to changing precipitation timing, phase and magnitude, growing season length, and vegetation snow and rain interactions.

Keywords: Evapotranspiration, surface energy balance, boreal forest, subalpine taiga, Shrubification, vegetation change

1 Introduction

The arctic and subarctic are rapidly warming, resulting in well documented and accelerating hydrological changes across the circumpolar north (Bring et al., 2016; Hinzman et al., 2020). While the impacts of warming cause cascading hydrological and ecological impacts that include degrading permafrost (Walvoord and Kurylyk, 2016), declining glaciers (Zemp et al., 2019), and changes to precipitation quantity, timing and phase (DeBeer et al., 2016, 2020), the most immediate ecosystem response is alteration to vegetation community composition density, distribution, and phenology (Bjorkman et al., 2020; Danby and Hik, 2007; Davis et al., 2020; Hinzman et al., 2013; Myers-Smith et al., 2017, 2020). Specifically, warmer temperatures have allowed the expansion of shrubs, a process termed shrubbification, across high latitude ecosystems (Chapin et al., 1995; Lantz et al, 2010b, 2013; Moffat et al., 2016; Myers-Smith and Hik, 2017; Post et al., 2009; Tape et al., 2006, 2012; Tremblay et al., 2012; Walker et al., 2006). In addition, trends of treeline advancement and infilling at high latitudes have also been documented (Conway and Danby, 2014; Harsch et al., 2009; Lloyd and Fastie, 2003), yet patterns are varied and mediated by species specific traits, reproduction rates, and environmental conditions at both landscape and local scales (Danby and Hik, 2007; Myers-Smith et al., 2020).

Changes in vegetation type and structure result in complex soil-plant-atmosphere feedbacks that alter how catchments collect, store and release water, which directly impacts the global climate cycle through the albedo feedback and energy partitioning (Bonan, 2008; Chapin et al., 2005; Lafleur and Humphreys, 2018; Sturm et al., 2005). For example, snow and rainfall accumulation and interception are strongly dependent upon vegetation type, height and density (Pomeroy et al., 2006; Sturm et al., 2001; Van Dijk et al., 2015; Zwieback et al., 2019). Leaf area controls rain and snow interception in northern boreal forests (Hedstrom and Pomeroy, 1998), whereas increases in shrub height enhances snow trapping (Pomeroy et al., 2006). Shrubs can also play a substantial role in rainfall interception, although this process is dependent on plant height and density. For example, Zwieback et al. (2019) found a 15-30% reduction in effective rainfall under birch shrubs, but reduced interception under alder. Vegetation influences the surface energy balance, affecting the rate and timing of snowmelt and evapotranspiration (ET) (Brummer et al., 2012; Kasurinen et al., 2014; Lafleur and Humphreys, 2018). Tall shrubs accelerate melt through the emission of long-wave radiation (Marsh et al., 2010; Pomeroy et al., 2006) despite

reducing turbulent fluxes (Endrizzi et al., 2010). Northern forests have distinct melt regimes from the dominance of shading and sheltering processes and often retain snow for longer periods, despite having an overall lower above-canopy albedo (Bonan, 2008). During the snow-free period, vegetation phenology controls energy partitioning and the ratio of evaporation to transpiration (Wang et al., 2014). Other widely identified impacts of northern vegetation change are to ground thermal and moisture regimes (Domine et al., 2016; Myers-Smith and Hik, 2013; Paradis et al., 2016; Sturm et al., 2005; Wilcox et al. 2019), carbon and nutrient cycling (Lafleur and Humphreys, 2018) and terrain stability (Lara et al., 2016). These critical zone feedback processes are complicated by dynamic and changing vegetation covers, both through "greening" of northern ecosystems from climate change and increasing risk of fire (Lantz et al., 2010). While the literature on surface-atmosphere interactions has grown in recent decades, current understanding of these hydrological interactions along a vegetation gradient does not: (1) represent alpine environments and (2) has been primarily focused on surface energy partitioning (i.e. Beringer et al., 2005). Therefore, the net impact of alpine shrub proliferation and treeline advance on the critical zone water balance remains unclear.

As northern ecosystems change, there is increasing pressure on water managers, First Nations and other stakeholders to understand and adapt to future water resources. As river regimes shift from declines in the cryosphere and changes in weather and climate (IPCC, 2019), the additional pressures of transitioning ecosystems must be assessed as ET strongly influences water partitioning in relatively dry, northern ecosystems. However, predicting ET over large scales is challenging, particularly in cold, alpine environments where observations are sparse and landscapes are heterogeneous (Bring et al., 2016). The objective of this paper is to advance our understanding of surface energy partitioning and ET dynamics across an ecological functional gradient within a heterogeneous, subarctic, alpine watershed. This provides a unique opportunity to compare the potential impacts of shifting ecosystem types within a local geographic area. Here, we present six years of observations of surface-atmosphere interactions from three subarctic sites across a thermal gradient and varying vegetation cover spanning boreal forest to sub-alpine taiga. Specifically, among a (1) white spruce forest, (2) tall, dense shrub and (3) short, sparse shrub sites, this paper compares seasonal and inter-annual surface energy partitioning ET

dynamics. We subsequently highlight the role of shifting vegetation on the water balance across this gradient and discuss the hydrological implications of ecosystem change in northern alpine catchments.

2. Methods

2.1. Study Sites

Wolf Creek Research Basin (WCRB) is located in Yukon Territory, Canada (~60.5˚N), 15 km south of the city of Whitehorse and within the southern Yukon River headwater region (Fig. 1). WCRB is located in the traditional territories of the Kwanlin Dün, Ta'an Kwäch'än Council and Carcross/Tagish First Nations. The drainage area of the basin is approximately 179 km^2 with elevation ranging between 660 and 2080 meters above sea level (masl) (Rasouli et al., 2019a). The climate of the basin is subarctic continental (Köppen Dfc), and the long term mean annual air temperature is 0.2°C as measured at the Whitehorse Airport (706 masl, Environment Canada, 1981-2010), and declines with elevation. The long-term Whitehorse precipitation average is 282 mm (Environment Canada, 1981-2010), yet this increases with elevation and can reach > 400 mm in WCRB in certain years (Carey et al., 2013; Rasouli et al., 2019a) The basin is composed of three distinct ecozones: boreal forest (22%) at lower elevations, subalpine taiga (58%) and alpine tundra (20%) (Rasouli et al., 2019a) (Fig. 1). The geology is sedimentary sandstone, siltstone, limestone and conglomerate with thick stony till and glacial drift above the bedrock for most of the basin. Sporadic and discontinuous permafrost occurs at high elevations and on north-facing slopes above treeline (Lewkowicz and Endie, 2004).

Three study sites were selected along an altitudinal gradient to represent the dominant vegetation and are termed: Forest, Buckbrush and Sparse Shrub. Forest is located near the WCRB outlet, at an elevation of 743 masl (Fig. A; Table 1). The canopy is composed primarily of White Spruce *(Picea glauca)*, approximately 12-20 m in height. Buckbrush is a subalpine taiga site located at mid-elevation (1250 masl). Vegetation consists of willow (*Salix*) and dwarf birch (*Betula nana*) shrubs, with mean heights of 1.24 ±0.33 and 0.83 ±0.45 m respectively. Sparse Shrub is a high-elevation (1425 masl) subalpine taiga site with shorter willow (*Salix*) and birch (*Betula nana*) cover and increased moss, lichen, and bare rock cover (Fig. 1). Mean height of willow and birch shrubs at Sparse Shrub is 0.55 ±0.3 m and 0.41 ±0.16 m respectively. Mean growing season leaf

area index (LAI) at Forest, Buckbrush and Sparse Shrub is 3.5, 2.5, and 1.7 m^2/m^2 (Table 1). Soil profiles at each site consisted of an organic layer of varying thickness atop primarily coarse sand with spatially variable compositions of gravel and silt.

2.2. Instrumentation

Fluxes of latent heat ($\lambda_v E$), sensible heat (H) and CO_2 were measured using the eddy covariance method at each site. Analysis presented here includes flux data year-round from 2017-2020 at Forest, and April to October from 2015-2020 at Buckbrush and Sparse Shrub. Each tower was instrumented with a 3-axis sonic anemometer and infrared gas analyzer (IRGA). A closed path LICOR-7200RS was installed at Forest and an open-path LICOR-7500A at the two shrub sites (Buckbrush and Sparse Shrub). All signals were scanned at a frequency of 10 Hz and recorded on a Campbell Scientific datalogger. Thirty-minute fluxes were computed from high frequency signals with EddyPro v 6.2.2 using block averaging, planer fit coordinate rotation (Wilczak, Oncley, and Stage, 2001), and WindMaster Pro vertical wind velocity correction multipliers. Soil temperature and moisture was measured at multiple depths at all sites from 2015 onwards, with soil water potential sensors (TEROS21) installed in June 2019 at all sites.

2.3. Data Processing, Gap-Filling and Energy Balance Closure

Open-path IRGA gas concentration density fluctuations were compensated using the Webb, Pearman, and Leuning correction (Webb et al., 1980). Both H_2O and CO_2 densities were directly output by the closed-path IRGA. Time lags were detected and compensated through covariance maximization. Spike detection and removal were computed according to Vickers and Mahrt (1997). Analytic correction for high-pass filtering effects were computed following Moncrieff et al. (2004) for all sites. Corrections for low-pass filtering effects were evaluated using methods by Moncrieff et al. (1997) for the open-path system and Horst (1997) for closed path. Fluxes were removed when turbulence was insufficient (friction velocity <0.1 m/s). Fluxes of $\lambda_v E$ and H were filled using artificial neural networks (ANNs) created with MATLAB (Mathworks Inc., Massachusetts,

USA) neural network toolbox. When data was available, $\lambda_v E$ and H were modeled using net radiation, vapour pressure deficit (VPD), wind speed, downward shortwave radiation, and air temperature. Mean coefficients of determination for the gap-filled $\lambda_v E$ data were 0.82 at Forest, 0.76 at Buckbrush, and 0.76 at Sparse Shrub (Table S1). Remaining gaps in data were filled using the mean diurnal variation method (Falge et al., 2001), replacing missing values with the mean for that time over the previous and subsequent 7-day period. Missing data from May to September for each tower are summarized in Table S1 with mean values of 35, 30 and 41% missing at Forest, Buckbrush and Sparse Shrub respectively. Periods of missing data were primarily at night and during periods of rain. Mean energy balance closure over the study period was 0.86, 0.74, 0.80 at Forest, Buckbrush and Sparse Shrub respectively (Table S1). Canopy heat storage at Forest was estimated using iButtons placed along the height of the tower at 2 m intervals and was estimated as 1% of net radiation (R_n).

3. Results

3.1. Climate

Climate results are confined from May to September for inter-comparison purposes and direct comparisons will be made from 2017 to 2020 when all sites were operational, unless otherwise stated. Average air temperature at the study sites decreased with increasing elevation, with mean May to September air temperatures of 11.1, 8.2, and 7.2°C at Forest, Buckbrush and Sparse Shrub respectively (Fig. 2; Table 2). The coolest year was 2020, when air temperatures were 0.8, 1.0, and 0.8°C lower than the mean at Forest, Buckbrush and Sparse Shrub respectively. The warmest year was 2019 when air temperatures 0.9, 1.0, and 1.2°C above the mean (Table 2). At all sites, mean monthly air temperature peaked in July (Fig. 2).

Total days per year with average air temperature above 0°C decreased with elevation; Forest averaged 222 days (±3), while Buckbrush and Sparse Shrub averaged 173 (±12) and 168 (±10) days. May to September precipitation (2017-2020) averaged 166 (±38) mm at the Forest compared to 228 (± 47) mm at the higher elevation sites. This compares to the 30-year climate normal (1981-2010) of 156 mm recorded 14 km north of the Forest site at the Whitehorse Airport (Environment Canada,

2021). At all sites, 2020 was the wettest with 325 mm rainfall at the shrub sites and 228 mm at Forest from May to September. The driest year was 2018, with 132 and 182 mm received at the forest and shrub sites respectively. Growing season length was defined as the number of days where net ecosystem exchange (NEE) was < 0 g C m^2 over a 24-hour period. Between 2017 and 2020, mean growing season length was 175 (±15) days at Forest, 139 (±18) days at Buckbrush, and 107 (±15) days at Sparse Shrub. The shortest growing season was 2020, with 154, 127, and 89 days at Forest, Buckbrush and Sparse Shrub respectively

3.2. Soil Moisture

Soil moisture patterns were consistent among years and sites, with volumetric water content (VWC) greatest immediately after snowmelt followed by a gradual decline and intermittent responses to rain events throughout the year (Fig. 3). Using 2019 as an example when both VWC and suction were measured, VWC was consistently highest at Buckbrush throughout the upper soil profile, followed by the Sparse Shrub and Forest soils (Fig. 3). There was considerable difference in VWC between the Forest and shrub sites as soils were consistently drier throughout the year at Forest and had muted responses to melt and rainfall. Soil matric potential sensors indicated that despite fluctuation in VWC with rainfall, soil tension at Buckbrush and Sparse Shrub never fell below -25 kPa, despite long periods without rain later in the year. In contrast, Forest soil tension was much lower, with near surface suctions falling below -30 kPa and 15 cm suctions below -90 kPa, while soil tensions at 30 cm fell below -2500 kPa later in the summer, far below the average wilting point for plants (-1500kPa).

3.3. Surface Energy Dynamics

3.3.1. Albedo

The partitioning of available energy varied within and among years. During the middle growing season (June to August), albedo was similar among sites, although values increased with increasing elevation and decreasing vegetation height, with mean mid-day (11:00-14:00) albedo of 0.09, 0.12 and 0.15 at the Forest, Buckbrush and Sparse Shrub, respectively (Fig. 4). At Forest, albedo was relatively consistent, ranging from 0.08 in July to a maximum of 0.21 in December. In contrast, intra-

and inter-annual variability was large at the shrub sites, where peak mean daytime albedo during the snow-covered months was 0.50 at Buckbrush and 0.82 at Sparse Shrub. Although the dominant species cover at Buckbrush and Sparse Shrub were similar, Birch and Willow shrubs were on average 0.42 and 0.79 m taller at Buckbrush than Sparse Shrub. This increased net radiation (R_n) during snowmelt and the initial snow-covered period in the fall (Fig. 4).

3.3.2. Energy Partitioning

The partitioning of energy among the study years showed marked yet consistent variability among sites (Fig. 4). On average, R_n peaked in June at Forest and May at both shrub sites, although there were subtle differences among sites, particularly the shrubs, where maximum R_n could occur in later summer months. All sites had a higher sensible heat flux (H) early in the season and then shifted to more $\lambda_v E$ dominated as the season progressed (Fig. 4). The transition from H to $\lambda_v E$ occurred later in the year with increasing elevation, on average occurring on May 31, June 14 and June 29 at Forest, Buckbrush and Sparse Shrub respectively. From May to September, mean $\lambda_v E/R_n$ at Forest was 0.47 (± 0.01), while $\lambda_v E /R_n$ was similar between Buckbrush and Sparse Shrub with $\lambda_v E /R_n$ of 0.31 (±0.02 and ±0.04) respectively (Table 2). Generally, variability in all interannual energy balance terms increased with elevation and reduced vegetation (Table 2; Fig. 4). The enhanced variability in energy partitioning (both annual and monthly) at the Sparse Shrub was highlighted in the dry 2018 when May to September $\lambda_v E /R_n$ dropped to 0.27, while $\lambda_v E /R_n$ at Buckbrush was 0.32. Partitioning of R_n to H was similar between Buckbrush and Sparse Shrub, with H/R_n of 0.41 (± 0.05 and 0.04) respectively, while at Forest, H/R_n was 0.45 (± 0.01). Ground heat flux (G) was highest at Sparse Shrub, peaking in May and mean G/R_n of 0.06 from May to September. G was low throughout the entire year at Forest and Buckbrush, with G/R_n of ~0.01.

3.4. ET Dynamics

Annual growing season ET declined with increasing elevation, while interannual variability increased. Mean May to September ET totals were 349 (±3) mm, 249 (±10) mm, and 240 (±26) mm at Forest, Buckbrush and Sparse Shrub respectively (Fig. 5; Table 2). At Forest, cumulative ET was consistent among the four years of study, regardless of growing season rainfall.

The Sparse Shrub site had the greatest year-to-year variability compared to Buckbrush, where cumulative ET was relatively more consistent (Fig. 5). From 2015-2020 at the shrub sites, total growing season ET was highest in the 2016, with cumulative ET higher at Sparse Shrub (285 mm) than Buckbrush (261 mm). This year had slightly higher mean May to September air temperature and rainfall (Table 2). Conversely, in the driest year (2018), where the shrub sites only received 182 mm of rainfall, we observed the lowest amount of ET at the Sparse Shrub (192 mm), while ET at Buckbrush was close to the interannual mean of 236 mm. Although 2020 was very wet, receiving 62 mm and 97 mm more rainfall than average from May to September, cumulative ET losses at all sites were close to the mean over the study years. Ratios of May to September ET to rainfall (ET:R) (Table 2) were the highest and most variable at Forest with mean ET:R of 2.19 (±0.37) compared to 1.22 (±0.09) and 1.14 (±0.05) at Buckbrush and Sparse Shrub respectively. The decrease in variability with increasing vegetation cover is also apparent seasonally.

The overall pattern of ET was more dynamic on a seasonal basis at the shrub sites, reflecting plant growth and senescence, with notable declines in ET rates between August and September (Fig. 5, 6). Comparatively, daily ET at Forest was more consistent between months, increasing in spring with a gradual decline in September. Daily ET peaked in July at all sites, with 2017-2020 mean July ET rates of 3.05 (±0.17), 2.48 (±0.09), and 2.13 (±0.31) mm/day (Fig.6). The largest difference between mean monthly ET rates between Forest and the two shrub sites occurred in June (Forest rates 1.0 mm/day greater than Buckbrush, and 0.9 mm/day greater than Sparse Shrub), while the largest difference between Buckbrush and Sparse shrub occurred in July during the peak growing season (Buckbrush ET rates greater by 0.35 mm/day). In all other months, mean ET rates at the shrub sites were similar, with differences less than 0.17 mm/day. Moving 14-day mean daily ET rates (Fig. 6) show larger variability at the Sparse Shrub site than Buckbrush or Forest, particularly early in the season. Variability in ET rates among years was lowest in the late growing season at all sites (early August).

4. Discussion

4.1. Influence of changing vegetation cover on energy partitioning

Small decreases in albedo will have a considerable positive impact on atmospheric temperatures, even with modest shifts in the landscape (Bonfils et al., 2012; Chapin et al., 2005). In all seasons, albedo at the Forest was lower than the Buckbrush and Sparse Shrub sites, and the difference between winter and summer was low (Fig. 4); a characteristic of boreal forests (Betts et al., 1997). Mean mid-day snow-free albedo of Buckbrush (0.12) was slightly lower than Sparse Shrub (0.15), which was similar to shrub and shrub taiga sites reported at a number of northern sites (Beringer et al., 2005; Eugster et al., 2000; Lafleur and Humphreys, 2018; Williamson et al., 2016). Unlike Williamson et al. (2016), who suggested an increase in albedo along a successional gradient in Yukon Territory, we observed a more widely reported decline in albedo with increased abundance and height of shrubs during the snow-free season.

Important feedbacks from future vegetation shifts on energy partitioning occurs during winter and the melt/accumulation season (Bonfils et al., 2012). The influence of shrub height and emergence during melt on snow accumulation, albedo and the energy balance has been well documented in northern environments (Bewley et al., 2010; Marsh et al., 2010; Menard et al., 2012; Pomeroy et al., 2006). When considering early season surface energy balances in varying shrub cover, the abundance of exposed branches controls albedo, which is dependent on the amount of snow, wind redistribution, the plasticity of woody stems and importantly, shrub height (Sturm et al., 2005). For low-stature shrubs (<0.6 m), Lafleur and Humphreys (2018) found no difference in late winter/spring albedo. Here however, differences in peak-winter albedo between shrub sites were large (0.5 at Buckbrush and 0.82 at Sparse Shrub), similar to results of Sturm et al. (2005) who reported mid-winter albedo of 0.85 for snow-covered shrubs and 0.6 when exposed. While the interplay between snow burial and shrub height varies regionally across the pan-arctic, in all cases, shifts in vegetation that act to increase shrub height and abundance will lower albedo, as well the encroachment of forests, with global radiative impacts considering the current rate of ecosystem change.

The influence of vegetation on energy partitioning of turbulent fluxes has highlighted differences between shrub and forest species across a range of environments (Eaton et al; 2001; Eugster et al., 2000; Kasurinen et al., 2014). With respect to shrubs, extent and wetness play a significant role, whereas for forests the role of leaf area index, meteorological conditions, and physiological regulation by vegetation and the distinction between conifer and deciduous species has been highlighted (Brümmer et al., 2012, Kasurinen et al., 2014). While synthesis studies provide important information on partitioning controls, generalizations occur due to the large variability in climate across northern biomes. There have been few studies comparing vegetation assemblages in the same hydroclimatological regime over several years, with the most similar study that of Beringer et al. (2005) who compared surface energy partitioning over one growing season at nearby sites in Alaska among tundra, shrubs and boreal forests. They reported that the greatest increases in H was between tall shrubs and forest, but not between tundra and tall shrubs, which is similar to our sites in that there was less difference in the magnitude and timing of energy partitioning among the shrub and Forest sites. While mean H was greater at the Forest, the relative partitioning of turbulent energy favoured $\lambda_v E$ in all years (Table 2). This is in contrast to Beringer et al. (2005) who report higher partitioning of available energy to H, with a Bowen ratio (β) of 1.22 from June to August at their white spruce site in one year compared to our average of 0.94 over four years. At Forest, there was a gradual decline and stabilization in β throughout the growing season, where in contrast, β at the shrub sites was much more variable on an annual basis and controlled by vegetation phenology (Fig. S1), with higher β occurring in the shoulder season when vegetation was not transpiring. While mean May to September β was similar between Buckbrush and Sparse Shrub (1.32 ±0.13 and 1.34 ±0.26) (Table 2) among years, seasonal variability in β was larger at Buckbrush than Sparse Shrub, with higher β in May and lower β in the mid-growing season . Whereas there is equivocal evidence as to how height and abundance affects $\lambda_v E$ and total water loss (Lafleur and Humphreys, 2018), our results suggest encroachment of woody vegetation will likely result in an increased β early in the year, and lower β in mid-growing season. However, the change in net radiation, seasonality of vegetation growth, nature of precipitation delivery, and physiological response will all control total evaporative losses, despite shifts in ratios of turbulent fluxes. The hydrological implications for this, discussed below, are that transitions in vegetation cover in WCRB will likely enhance water loss through an increase in ET despite increases in H.

4.2. Hydrological Implications of Vegetation Change

While research indicates that increased terrestrial productivity in northern environments will increase ET (Bring et al., 2016; Rawlins et al., 2010; Zhang et al., 2009), there is limited empirical data as to how treeline advance and shrub height and abundance affect ecosystem ET and other components of the hydrological cycle. Our results are similar to those that showed negligible differences in ET between shrubs of different heights (Chapin et al., 2000; Lafleur and Humphreys, 2018; McFadden et al., 2003). However, while seasonal totals were similar, there were distinct processes operating that distinguished the two shrub sites. Diurnal monthly traces of ET and net ecosystem exchange (NEE) (Fig. 7) suggest that during July, increased ET at Buckbrush is driven by enhanced transpiration as reflected by the greater NEE compared with Sparse Shrub, which has more modest mid-season NEE. However, during May, when photosynthesis/transpiration was low, the Sparse Shrub site has greater ET, most likely driven by enhanced direct soil evaporation as there is much more exposed bare ground. These offsetting processes result in annual ET totals being similar, yet the reduced influence of vegetation at the Sparse Shrub site increases ET variability. During wet years, ET is similar between Buckbrush and Sparse Shrub, yet during dry years such as 2018, the Sparse Shrub is notably lower. While shrubs can effectively utilize available soil moisture, sustaining high rates at Buckbrush where vegetation coverage is dense, bare ground evaporation at Sparse Shrub becomes suppressed during dry periods, lowering overall ET. Of note, the length of growing season did not influence total ET between the two shrub sites (Fig. 3), again supporting the role of bare ground evaporation at the Sparse Shrub site.

Although warmer temperatures and a longer growing season partly explain greater total ET at Forest than the shrub sites (Fig. 7), physiological and ecosystem processes help explain enhanced water loss and low ET variability. Both Forest and Buckbrush have relatively low variability in ET rates among years, particularly later in the growing season (July/August) relative to the Sparse Shrub site (Fig. 6), highlighting a mediating effect of vegetation during the prime growing season. Monthly diurnal traces of ET and NEE from the three sites indicate that as soon as soils thaw in May, transpiration/photosynthesis begins at Forest, whereas at the shrub sites, ET/NEE in May is negligible before bud-burst in late May or early June (Fig. 7). Monthly mean ET rates at the Forest site are similar in June, July and August, while at the two shrub sites, the greatest difference in mean monthly daily ET occurs in July. Similar timing of senescence between both shrub

sites is apparent in lower ET rates and declines in carbon uptake. Physiologically, the forest is transpiring/photosynthesizing throughout the growing season at consistent rates, and while there are declines related to periods of low rainfall, the forest effectively uses available water. The role of vegetation in making ET a conservative process has been outlined in theoretical (Jarvis and McNaughton, 1986; Rodriguez-Iturbe and Porporato, 2007), and field studies (Oishi et al., 2010 Phillips and Oren, 2001; Roberts, 1983). Therefore, we assert that treeline advance and shrub proliferation will result in more stable, higher ET rates that are less responsive to inter-annual variation in precipitation compared to areas with shorter, less dense shrub cover. However, the total increase in ET from shrub infilling will be muted and increases primarily in the mid-growing season.

The nature of evaporative fluxes coupled with the timing, magnitude and phase of precipitation delivery has important implications for watershed scale hydrological processes. A critical implication of the higher ET at Forest is the increased ET:R and considerable water deficit from May to September (Fig. 5). This indicates the site is heavily reliant on snowmelt recharge and potentially late season rains to sustain high ET (ET:R = 2.19) rates compared with the shrub sites where there is less evident moisture limitation (ET:R =1.20 and 1.14 at Buckbrush and Sparse Shrub respectively). In a synthesis of northern watersheds, Tetzlaff et al. (2013) suggest that with climate change, catchments will move towards increasing aridity as ET increases at a rate greater than precipitation. However, in this region, total precipitation is expected to increase with enhanced rainfall contributions (IPCC, 2019; Tetzlaff et al., 2013). Climate and vegetation change modelling by Rasouli et al. (2019b) in WCRB suggest that at higher elevations, increased in snow trapping due to higher stature shrubs will likely offset the decrease in snow water equivalent due to climate change. This compensation does not, however, apply to boreal forest covers at low elevations. Considering the large growing season water deficit and drier soils, decreases in snow input early in the season or more periods of extreme weather (and potentially drought) could push the Forest into a situation of moisture stress. The growth of white spruce forests in areas of low precipitation and rapid warming is known to be limited due to water deficits, and future climate change may cause higher tree mortality in these populations in high latitudes of North America (Hynes and Hamann, 2020).

We found the primary hydrological difference between shrub sites was during the mid-growing season (Fig. 7), although on an annual timescale over six years there does not appear to be a large difference in ET when shrubs increase in height and density. This may change as warming alters the timing of snowmelt and growing season length, resulting in a longer "mid-season" difference between shrub covers of varying height. The greater influence is the enhanced snow trapping associated with shrub growth (Pomeroy et al., 2006; Rasouli et al., 2019b), which will enhance recharge and runoff generation, particularly during freshet.

4.3. Considerations for predicting future hydrologic regimes in northern regions

Despite accelerating research in the north and a new dominance of remote sensing and model-based outcomes at the expense of empirical data, there remains a nascent understanding of how integrated environmental changes will alter the storage and cycling of water in cold regions. While hydrological changes are most often ascribed to warmer air temperatures and changes in frozen ground status at larger scales (Walvoord and Kurylyk, 2016), the influence of changing vegetation communities on hydrological storage and flux remains uncertain as there have been few studies showing only modest influences. There has been considerable research documenting rapid vegetation change, particularly the advance of tree-dominated communities into tundra ecosystems (Danby and Hik, 2007; Conway and Danby, 2014; Harsch et al. 2009; Lloyd and Fastie, 2003) and the proliferation of tall shrubs into low tundra (Myers-Smith and Hik, 2017; Tape et al., 2006; Tremblay et al., 2012). Feedbacks from shrub expansion include enhanced snow trapping, warming soils, and enhanced nutrient availability, all of which enhance further shrub growth and potential for tree establishment (Myers-Smith et al., 2011; Sturm et al., 2001). The timescales of these changes must be considered, however, in future hydrological projections as treeline advance and infilling is slow (Danby and Hik, 2007) compared with rapid increases in shrub extent, density and height (Myers-Smith et al., 2011; Tape et al., 2006). These changes are also highly dependent on permafrost thaw and disturbances such as fire, which are expected to continue increasing in rate in coming decades (Lantz et al., 2010a). This will, to varying degrees, start new successional shifts depending on the severity and may result in more deciduous forest rather than boreal conifer species.

To our knowledge, there has been no documentation of surface energy and evaporative fluxes across a northern alpine watershed over multiple years. From an ET perspective, increased forest abundance and shrub proliferation will lead to changing soil moisture regimes and runoff timing and volume. Specifically, increases in ET will reduce runoff generation, particularly in the growing season. For WCRB, most of the streamflow is generated in the alpine and subalpine zone, and upward expansions of trees would reduce total catchment yield. While increase shrubs may trap more snow and provide more water during freshet, mid-season flows are expected to become less variable and decline with increasing shrub abundance.

Perhaps the greatest challenge in understanding the role of vegetation change on catchment hydrology is the role of precipitation. Changes from snow to rain, enhanced periods of drought or intense precipitation, all of which are predicted for pan-Arctic ecosystems (IPCC, 2019), will have profound effects on runoff regimes. While ET is a large flux, increased vegetation will likely reduce its variability, emphasizing the role of future precipitation uncertainty in watershed scale hydrological processes. The role of interception on total ET is an area for additional research to evaluate the relative impact of plant structure and physiology. While Zweibeck (2019) suggested that shrub interception reduced below canopy rainfall by 15-30% for shrub species, the role of rainfall interception has not been directly evaluated in this environment. We have a much greater understanding on how vegetation influences snow processes than rainfall processes in cold environments, but the large LAI and relatively open canopy suggests that rainfall interception at the Forest is considerable.

Conclusion

The impact of vegetation change on energy and water cycling in the pan-Arctic is an area of intense research, with literature syntheses (Bring et al., 2016; Wrona et al., 2016), numerical model outputs (Rawlins et al., 2010), and remote sensing (Zhang et al., 2009) suggesting ET will increase from increased air temperature, VPD, precipitation, a longer growing season and an expansion of shrubs and trees. There remains, however, few field-based studies that directly evaluate these processes in northern ecosystems. In this multi-year study, we highlight differences and similarities in the timing and magnitude of energy and mass fluxes among boreal forest and shrub taiga ecosystems in an alpine environment where elevation controls temperature and moisture regimes. Results indicate that the greatest change in water and energy fluxes will

occur from changes in treeline compared with shrubification across all seasons as they have distinct regimes. ET was greatest at the Forest site compared with the shrub sites, and varied little over 4 years despite differences in meteorology and a considerable growing season water deficit. In contrast, ET was considerably less at the cooler higher elevation shrub sites, which exhibited similar ET losses over 6 years despite differences in shrub height and abundance. While the observation of limited differences in ET has been reported before for a single year, our results indicate that ET variance is much greater at the short, sparse shrub site compared with the tall, dense shrub site due the reduced influence of vegetation controls on total ET. While there are multiple interacting processes, our results support the assertion that a greening north will have lower albedos and higher ET losses. How this affects catchment response will be strongly influenced by precipitation timing, phase and magnitude, growing season length, and vegetation snow and rain interactions.

Data Availability

Data will be made available to reviewers upon request and made publicly available upon acceptance of this manuscript. We are willing to provide all data and code to reviewers of this manuscript and upon request in HESS-D. However, as the study site is located on the traditional territories of three Canadian First Nations, provisions under the Ownership, Control, Access and Possession guidelines must be adhered to (see http://fnigc.ca/ocap-training/ for information). Upon acceptance of this manuscript, a DOI will be created for the final submission and the data stored in https://www.frdr-dfdr.ca/ where previous data from Wolf Creek Research Basin has been deposited.

Author Contributions

EN performed the data quality control, formal analysis and wrote the original draft of the article. SC reviewed and edited the final draft.

Competing Interests

The authors declare that they have no conflict of interest.

Acknowledgements

Authors would like to thank Dr. Gordon Drewitt for initial data processing, Dr. Michael Treberg for instrument maintenance and calibration and Tyler de Jong, David Barrett, and Dr. Nadine Shatilla for field assistance. We acknowledge the continued support of the Water Resources Branch, Government of Yukon, for the operation of Wolf Creek Research Basin. Financial support was provided by the National Science and Engineering Council of Canada through Discovery Grants and the Changing Cold Region Network, the Global Water Futures Program and the Weston Family Foundation.

425

References

Beringer, J., Chapin, F.S. III, Thompson, C.C., McGuire, A.D., 2005. Surface energy exchanges along a tundra-forest transition and feedbacks to climate. Agric. For. Meteorol. 131, 143-161.

430 Betts, A. K., Ball, J. H., 1997. Albedo over the boreal forest. J. Geophys. Res. 102(D24), 28901– 28909, doi:10.1029/96JD03876.

Bjorkman, A.D., García Criado, M., Myers-Smith, I.H., Ravolainen, V., Jónsdóttir, I.S., Westergaard, K.B., Lawler, J.P., Aronsson, M., Bennett, B., Gardfjell, H., Heiðmarsson, S., Stewart, L., Normand, S., 2020. Status and trends in Arctic vegetation: Evidence from experimental warming and long-term monitoring. Ambio. 49, 678–692, doi:10.1007/s13280-019-01161-6.

Bonan, G.B., 2008. Forests and Climate Change: Forcings, Feedbacks, and the Climate Benefits of Forests. Science 320(5882), 1444-1449, doi:

435 10.1126/science.1155121.

Bonfils, C.J.W., Phillips, T.J., Lawrence, D.M., Cameron-Smith, P., Riley, W.J., Subin, Z.M. 2012. On the influence of shrub height and expansion on northern high latitude climate. Environ. Res. Lett. 7, 015503, doi:10.1088/1748-9326/7/1/015503.

Bring, A., Fedorova, I., Dibike, Y., Hinzman, L., Mård, J., Mernild, S.H., Prowse, T., Semenova, O., Stuefer, S.L., Woo, M.K., 2016. Arctic terrestrial hydrology: A synthesis of processes, regional effects, and research challenges. J. Geophys. Res. Biogeosci. 121, 621–

440 649, doi:10.1002/2015JG003131.

Chapin, F., Shaver, G., Giblin, A., Nadelhoffer, K., Laundre, J., 1995. Responses of Arctic Tundra to Experimental and Observed in Climate. Ecology. 76(3), 694-711, doi:10.2307/1939337.

Chapin, F.S., Sturm, M., Serreze, M. C., McFadden, J. P., Key, J. R., Lloyd, A. H., McGuire, A.D., Rupp, T.S., Lynch, A.H., Schimel, J.P, Beringer, J., Chapman, W.L., Epstein, H.E., Euskirchen, E.S., Hinzman, L.D., Jia, G., Ping, C.L., Tape, K.D., Thompson,

445 C.D.C., Walker, D.A., Welker, J.M., 2005. Role of land-surface changes in Arctic summer warming. Science 310(5748), 657-660.

Conway, A.J., Danby, R.K., 2014. Recent advance of forest ecotones in southwest Yukon grasslands. Can. J. For. Res. 44, doi: 10.1139 / cjfr-2013-0429,509-520.

Danby, R.K., Hik, D.S., 2007. Variability, contingency and rapid change in subarctic alpine tree line dynamics. J. Ecol. 95, 352 – 363.

Davis, E., Trant, A., Hermanutz, L., Way, R.G., Lewkowicz, A.G., Siegwart Collier, L., Cuerrier, A., Whitaker, D, 2020. Plant-Environment Interactions in the Low Arctic Torngat Mountains of Labrador. Ecosystems doi: 10.1007/s10021-020-00577-6.

DeBeer, C. M., Wheater, H. S., Carey, S. K., Chun, K. P., 2016. Recent climatic, cryospheric, and hydrological changes over the interior of western Canada: a review and synthesis. Hydrol. Earth Syst. Sci. 20, 1573–1598, https://doi.org/10.5194/hess-20-1573-2016.

DeBeer, C. M., Wheater, H. S., Pomeroy, J. W., Barr, A. G., Baltzer, J. L., Johnstone, J. F., Turetsky, M. R., Stewart, R. E., Hayashi, M., van der Kamp, G., Marshall, S., Campbell, E., Marsh, P., Carey, S. K., Quinton, W. L., Li, Y., Razavi, S., Berg, A., McDonnell, J. J., Spence, C., Helgason, W. D., Ireson, A. M., Black, T. A., Davison, B., Howard, A., Thériault, J. M., Shook, K., Pietroniro, A., 2020. Summary and synthesis of Changing Cold Regions Network (CCRN) research in the interior of western Canada – Part 2: Future change in cryosphere, vegetation, and hydrology. Hydrol. Earth Syst. Sci. Discuss. [preprint], https://doi.org/10.5194/hess-2020-491, in review.

Endrizzi, S., Marsh, P., 2010. Observations and modelling of turbulent fluxes during melt at the shrub-tundra transition zone 1: point scale variations. Hydrol. Res. 41(6), 471, doi: 10.2166/nh.2010.149.

Environment Canada., 2021. Canadian climate normals 1981–2010 station data. Government of Canada, Ottawa.

Eugster, W., Rouse, W.R., Pielke Sr, R.A., Mcfadden, J.P., Baldocchi, D.D., Kittel, T.G.F., Chapin, F.S., III, Liston, G.E., Vidale, P.L., Vaganov, E., Chambers, S., 2000. Land–atmosphere energy exchange in Arctic tundra and boreal forest: available data and feedbacks to climate. Glob. Change Biol. 6, 84-115, doi:10.1046/j.1365-2486.2000.06015.x.

Falge, E., Baldocchi, D., Olson, R. J., Anthoni, P., Aubinet, M., Bernhofer, C., Burba, G., Ceulemans, R., Clement, R., Dolman, H., Granier, A., Gross, P., Grünwald, T., Hollinger, D., Jensen, N., Katul, G., Keronen, P., Kowalski, A., Ta Lai, C., Law, B.E., Meyers, T., Moncrieff, J., Moors, E., Munger, J.W., Pilegaard, K., Rannik, Ü., Rebmann, C., Suyker, A., Tenhunen, J., Tu, K., Verma, S., Vesala, T., Wilson, K., Wofsy, S., 2001. Gap filling strategies for defensible annual sums of net ecosystem exchange. Agric. For. Meteorol. 107, 43–69, https://doi.org/10.1016/S0168-1923(00)00225-2.

Harsch, M.A., Hulme, P.E, McGlone, M.S, Duncan, R.P., 2009. Are treelines advancing? A global meta-analysis of treeline response to climate warming. Ecol. Let. 12, 1040-9, doi:10.1111/j.1461-0248.2009.01355.x.

Hedstrom, N.R., Pomeroy, J.W., 1998. Measurements and modelling of snow interception in the boreal forest. Hydrol. Process. 12, 1611-1625.

Hinzman, A.M., Sjöberg, Y., Lyon, S.W., Ploum, S.W., Velde, Y., 2020. Increasing non-linearity of the storage-discharge relationship in sub-Arctic catchments. Hydrol. Process. 34, 3894–3909, doi:10.1002/hyp.13860.

Hinzman, L.D., Deal, C.J., McGuire, A.D., Mernild, S.H., Polyakov, I.V., Walsh, J.E., 2013. Trajectory of the Arctic as an integrated system. Ecol. Appl. 23, 1837-1868. doi:10.1890/11-1498.1.

Horst, T. W., 1997. A simple formula for attenuation of eddy fluxes measured with first order response scalar sensors. Bound-Lay Meteorol. 82, 219–233, https://doi.org/10.1023/A:1000229130034.

Hynes, A., Hamann, A., 2020. Moisture deficits limit growth of white spruce in the west-central boreal forest of North America. Forest Ecol. Manag. 461, 117944.

IPCC, 2019. IPCC Special Report on the Ocean and Cryosphere in a Changing Climate [H.-O. Pörtner, D.C. Roberts, V. Masson-Delmotte, P. Zhai, M. Tignor, E. Poloczanska, K. Mintenbeck, A. Alegría, M. Nicolai, A. Okem, J. Petzold, B. Rama, N.M. Weyer (eds.)]. In press.

Jarvis, P. G., McNaughton, K. G., 1986. Stomatal control of transpiration: scaling up from leaf to region. Adv. Ecol. Res. 15, 1-49.

Lafleur, P., Humphreys, E.R., 2018. Tundra shrubs on growing season energy and carbon dioxide exchange. Environ. Res. Lett. 13, 055001.

Lantz, T.C., Gergel, S.E, Henry, G.H.R., 2010a. Response of green alder (Alnus viridis subsp fruticosa) patch dynamics and plant community composition to fire and regional temperature in north-western Canada. J. Biogeogr. 37, 1597–610.

Lantz, T.C., Gergel, S.E., Kokelj, S.V., 2010b. Spatial heterogeneity in the shrub tundra ecotone in the Mackenzie Delta region, Northwest Territories: implications for Arctic environmental Change. Ecosystems 13, 194–204.

Lantz, T.C., Marsh, P., Kokelj, S.V., 2013. Recent Shrub Proliferation in the Mackenzie Delta Uplands and Microclimatic Implications. Ecosystems 16, 47-59, doi: 10.1007/s10021-012-9595-2.

Lara, M.J., Genet, H., McGuire, A.D., Euskirchen, E.S., Zhang,Y., Brown, D.R.N., Jorgenson, M.T., Romanovsky, V., Breen, A., Bolton, W.R., 2016. Thermokarst rates intensity due to climate change and forest fragmentation in an Alaskan boreal forest lowland, Glob. Change Biol. 22, 816-829, doi:10.1111/gcb.13124.

Lewkowicz, A., Ednie, M., 2004. Probability Mapping of Mountain Permafrost Using the BTS Method, Wolf Creek, Yukon Territory, Canada. Permafrost Periglac. 15, 67-80, doi:10.1002/ppp.480.

Lloyd, A.H., Fastie, C.L., 2003. Recent changes in treeline forest distribution and structure in interior Alaska. Écoscience 10, 176-185, doi: 10.1080/11956860.2003.11682765.

Moffat, N.D., Lantz, T.C., Fraser, R.H., Olthof, I., 2016. Recent vegetation change 1980–2013 in the tundra ecosystems of the

Tuktoyaktuk Coastlands, NWT, Canada. Arct. Antarct. Alp. Res. 48, 581–597.

Moncrieff, J., Clement, R., Finnigan, J., Meyers, T., 2004. Averaging, detrending, and filtering of eddy covariance time series. In X. Lee, W. J. Massman, and B. Law (Eds.), Handbook of Micrometeorology, (pp. 7–31). Amsterdam The Netherlands: Springer Netherlands.

Moncrieff, J. B., Massheder, J. M., de Bruin, H., Ebers, J., Friborg, T., Heusinkveld, B., Kabat, P., Scott, S., Soegaard, H., Verhoef, A., 1997. A system to measure surface fluxes of momentum, sensible heat, water vapor and carbon dioxide. J. Hydrol. 188–189, 589–611.

Moore, R. D., Fleming, S.W., Menounos, B., Wheate, R., Fountain, A., Stahl, K., Holm, K., Jakob, M., 2009. Glacier change in western North America: influences on hydrology, geomorphic hazards and water quality. Hydrol. Process. 23, 42–61.

Mu, Q., Jones, L.A., Kimball, J.S., McDonald, K.C., Running, S.W., 2009. Satellite assessment of land surface evapotranspiration for the pan-Arctic domain. Water Resour. Res. 45, W09420, doi:10.1029/2008WR007189.

Myers-Smith, I., Kerby, J., Phoenix, G., Bjerke, J., Epstein, H., Assmann, J., John, C., Andreu-Hayles, L., Angers-Blodin, S., Beck, P., Berner, L., Bhatt, U., Bjorkman, A., Blok, D., Bryn, A., Christiansen, C., Cornelissen, J., Cunliffe, A., Elmendorf, S., Forbes, B.C., Goetz, S.J., Hollister, R.D., do Jong, R., Loranty, M.M., Macias-Fauria, M., Maseyk, K., Normand, S., Olofsson, J., Parker, T.C., Paramentier, F.W., Post, E., Schaepman-Strub, G., Stordal, F., Sullivan, P.F., Thomas, H.J.D., Tommervik, H., Treharne, R., Tweedie, C.E., Walker, D.A., Wilmking, M., Wipf, S., 2020. Complexity revealed in the greening of the Arctic. Nat. Clim. Chang. 10, 106-117, doi: 10.1038/s41558-019-0688-1.

Myers-Smith, I.H., Hik, D.S. 2017. Climate warming as a driver of tundra shrubline advance. J Ecol. 106, 547– 560, https://doi.org/10.1111/1365-2745.12817.

Myers-Smith, I.H., Forbes, B.C., Wilmking, M., Hallinger, M., Lantz, T., Blok, D., Tape, K.D., Macias-Fauria, M., Sass-Klaassen, U., L évesque, E., Boudrea, S., Ropars, P., Hermanutz, L., Trant, A., Siegwart Collier, L., Weijers, S., Rozema, J., Rayback, S.A., Schmidt, N.M., Schaepman-Strub, G., Wipf, S., Rixen, C., Ménard, C.B., Venn, S., Goetz, S., Andreu-Hayles, L., Elmendorf, S., Ravolainen, V., Welker, J., Grogan, P., Epstein, H.E., Hik, D.S., 2011. Shrub expansion in tundra ecosystems: Dynamics, impacts and research priorities. Environ. Res. Lett. 6(4), 045509.

Oishi, A. C., Oren, R., Novick, K. A., Palmroth, S., Katul, G. G., 2010. Interannual invariability of forest evapotranspiration and its consequence to water flow downstream. Ecosystems 13(3), 421-436.

Pomeroy, J.W., Bewley, D.S., Essery, R.L.H., Hedstrom, N.R., Link, T., Granger, R.J., Sicart, J.E., Ellis, C.R., Janowicz, J. R., 2006. Shrub tundra snowmelt. Hydrol. Process. 20, 923-941, doi:10.1002/hyp.6124.

Phillips, N., Oren, R., 2001. Intra-and inter-annual variation in transpiration of a pine forest. Ecol. Appl. 11(2), 385-396.

Post, E., Forchhammer, M. C., Bret-Harte, M. S., Callaghan, T. V., Christensen, T. R., Elberling, B., Fox, A.D., Gilg, O., Hik, D.S., Høye, T.T., Ims, R.A., Jeppesen, E., Klein, D.R., Madsen, J., McGuire, A.D., Rysgaard, S., Schindler, D.E., Stirling, I., Tamstorf, M.P., Tyler, N.J.C., van der Wal, R., Welker, J., Wookey, P.A., Schmidt, N.M., Aastrup, P., 2009. Ecological dynamics across the Arctic associated with recent climate change. Science 325(5946), 1355–1358, doi:10.1126/science.1173113.

Rasouli, K., Pomeroy, J.W., Janowicz, J.R., Carey, S.K., Williams, T.J., 2014. Hydrological sensitivity of a northern mountain basin to climate change. Hydrol. Process. 28, 4191-4208, doi: 10.1002/hyp.10244.

Rasouli, K., Pomeroy, J.W., Janowicz, J.R., Williams, T.J., Carey, S.K., 2019a. A long-term hydrometeorological dataset (1993-2014) of a northern mountain basin: Wolf Creek Research Basin, Yukon Territory, Canada. Earth Syst. Sci. Data. 11, 89-100, doi: https://doi.org/10.5194/essd-2018-118.

Rasouli, K., Pomeroy, J.W., Whitfield, P.H., 2019b. Are the effects of vegetation and soil changes as important as climate change impacts on hydrological processes? Hydrol. Earth Syst. Sci. 23, 4933 – 4954, https://doi.org/10.5194/hess-23-4933-20192019.

Rawlins, M. A., Steele, M., Holland, M., Adam, J., Cherry, J., Francis, J., Groisman, P., Hinzman, L., Huntington, T., Kane, D., Kimball, J., Kwok, R., Lammers, R., Lee, C., Lettenmaier, D., Mcdonald, K., Podest, E., Pundsack, J., Rudels, B., Maine, A., 2010. Analysis of the Arctic system for freshwater cycle intensification: Observations and expectations. J. Clim. 23(21), 5715–5737, doi:10.1175/2010JCLI3421.1.

Roberts, J., 1983. Forest transpiration: a conservative hydrological process? J. Hydrol. 66(1-4), 133-141.

Rodríguez-Iturbe, I., Porporato, A., 2007. Ecohydrology of water-controlled ecosystems: soil moisture and plant dynamics, Cambridge University Press.

Sturm, M., Douglas, T., Racine, C, Liston, G. E., 2005. Changing snow and shrub conditions affect albedo with global implications. J. Geophys. Res. Biogeosci. 110, G01004, doi:10.1029/2005JG000013.

Sturm, M., McFadden, J.P., Liston, G.E., Chapin III, S., Racine, C.H., Holmgren, J., 2001. Snow-Shrub Interactions in Arctic Tundra: A Hypothesis with Climatic Implications. J. Climate. 14, 336-344.

Tape, K. D., Sturm, M., Racine, C. H., 2006. The evidence for shrub expansion in Northern Alaska and the Pan-Arctic. Glob. Change Biol. 12, 686–702.

Tape, K., Hallinger, M., Welker, J., Ruess, R., 2012. Landscape heterogeneity of shrub expansion in Arctic Alaska. Ecosystems 15, 711–724.

Tremblay, B., Levesque, E., Boudreau, S., 2012. Recent expansion of erect shrubs in the Low Arctic: evidence from Eastern Nunavik, Environ. Res. Lett. 7, 035501.

Tremblay, B., Levesque, E., Boudreau, S., 2012. Recent expansion of erect shrubs in the Low Arctic: evidence from Eastern Nunavik, Environ. Res. Lett. **7**, 035501, doi:10.1088/1748-9326/7/3/035501.

Vickers, D., Mahrt, L., 1997. Quality control and flux sampling problems for tower and aircraft data. J. Atmos. Ocean. Tech. 14, 512–526, https://doi.org/10.1175/1520-0426.

Walker, M.D., Wahren, C.H., Hollister, R.D., Henry, G.H.R., Ahlquist, L.E., Alatalo, J.M., Syndonia Bret-Harte, M., Calef, M.P., Callaghan, T.V., Carroll, A.B., Epstein, H.E., Jónsdóttir, I.S., Klein, J.A., Magnússon, B., Molau, U., Oberbauer, S.F., Rewa, S.P., Robinson, C.H., Shaver, G.R., Suding, K.N., Thompson, C.C., Tolvanen, A., Totlandt, O., Turner, P.L., Tweedie, C.E., Webber, P.J., Wookey, P.A., 2006. Plant community responses to experimental warming across the tundra biome. P. Natl. A. Sci. 103, 1342-1346.

Walvoord, M.A., Kurylyk, B.L., 2016. Hydrologic Impacts of Thawing Permafrost – A Review, Vadose Zone Journal, 15(6), 1-20, doi:10.2136/vzj2016.01.0010.

Wang, L., Good, S.P., Caylor, K.K., 2014. Global synthesis of vegetation control on evapotranspiration partitioning. Geophys. Res. Lett., 41, 6753–6757, doi:10.1002/2014GL061439.

Webb, E. K., Pearman, G. I., Leuning, R., 1980. Correction of flux measurements for density effects due to heat and water vapour transfer, Q. J. Roy. Meteor. Soc. 106, 85–100, https://doi.org/10.1002/qj.49710644707.

Wilczak, J. M., Oncley, S. P., Stage, S. A., 2001. Sonic anemometer tilt correction algorithms. Bound-Lay. Meteorol. 99, 127–150, https://doi.org/10.1023/A:1018966204465.

Wrona, F.J., Johansson, M., Culp, J.M., Jenkins, A., Mard, J., Myers-Smith, I.H., Prowse, T.D., Vincent, W.F., Wookey, P.A., 2016. Transitions in Arctic ecosystems: Ecological implications of a changing hydrological regime. J. Geophys. Res. Biogeosci. 121, 650-674, doi:10.1002/2015.JG003133.

Zemp, M., Frey, H., Gärtner-Roer, I., Nussbaumer, S.U., Hoelzle, M., Paul, F., Haeberli, W., Denzinger, F., Ahlstr øm, A.P., Anderson, B., Bajracharya, S., Baroni, C., Braun, L.N., Cáceres, B.E., Casassa, G., Cobos, G., Dávila, L.R., Delgado Granados, H., Demuth, M., Espizua, L., Fischer, A., Fujita, K., Gadek, B., Ghazandar, A., Hagen, J.O., Holmlund, P., Karimi, N., Li, Z., Pelto, M., Pitte, P., Popovnin, V.V., Portocarrero, C.A., Prinz, R., Sangeware, C.V., Severskiy, I., Sigurdsson, O., Soruco, A., Usubaliev, R., Vincent, C., 2015. Historically unprecedented global glacier decline in the early 21st century. J. Glaciol. 61(228), 745-762, doi:10.3189/2015JoG15J017.

Zhang, K., Kimball, J.S., Mu, Q., Jones, L.A., Goetz, S.J., Running, S.W., 2009. Satellite based analysis of northern ET trends and associated changes in the regional water balance from 1983 to 2005. J. Hydrol. 379(1), 92–110.

Zwieback, S., Chang, Q., Marsh, P., Berg, A., 2019. Shrub tundra ecohydrology: rainfall interception is a major component of the water balance. Environ. Res. Lett. 14, 055005, doi:10.1088/1748-9326/ab1049.

Figures

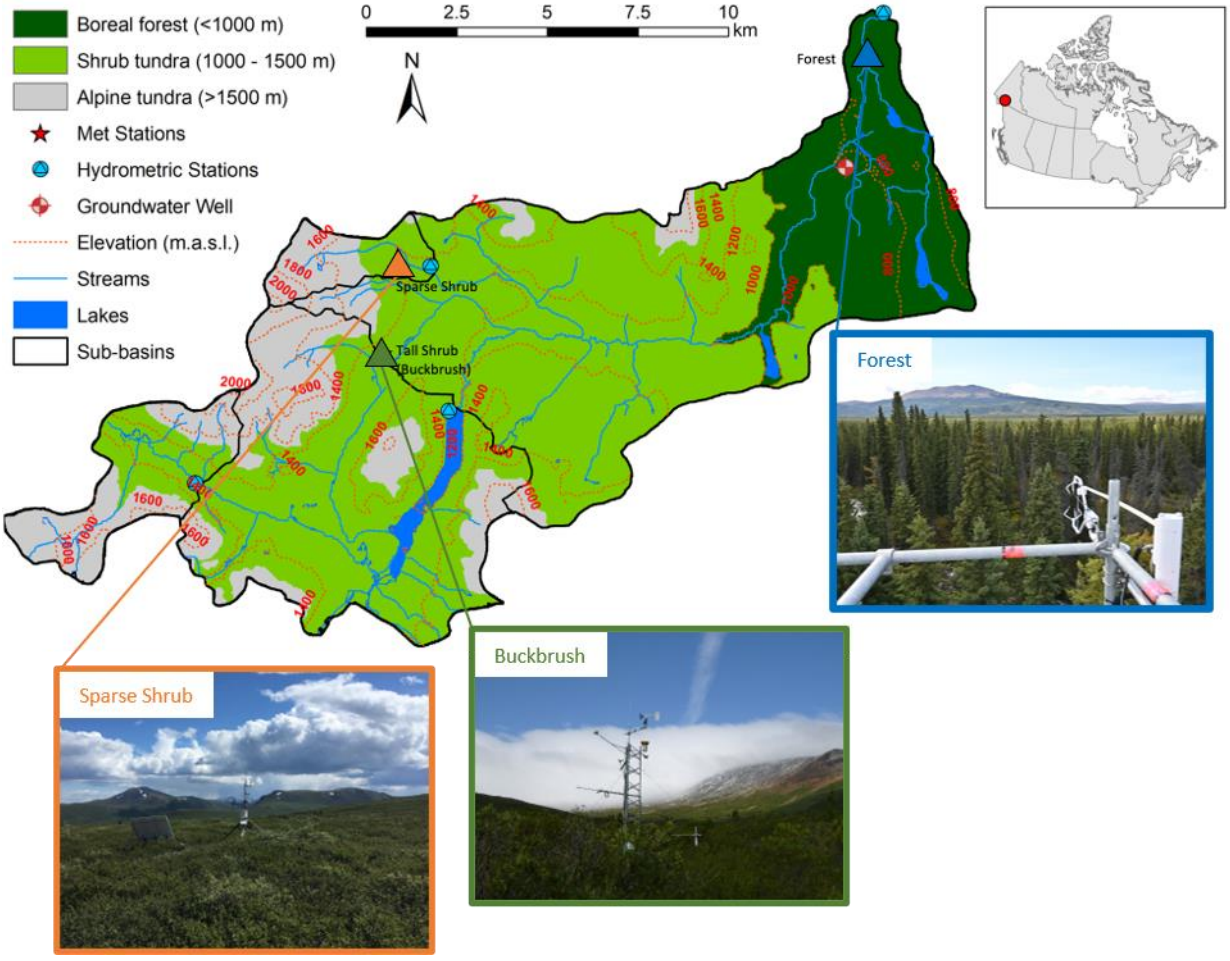

Figure 1: Map of Wolf Creek Research Basin showing vegetation cover, elevation, stream network, and tower locations. Insets are photos of Forest, Buckbrush, and Sparse Shrub taken in July.

595

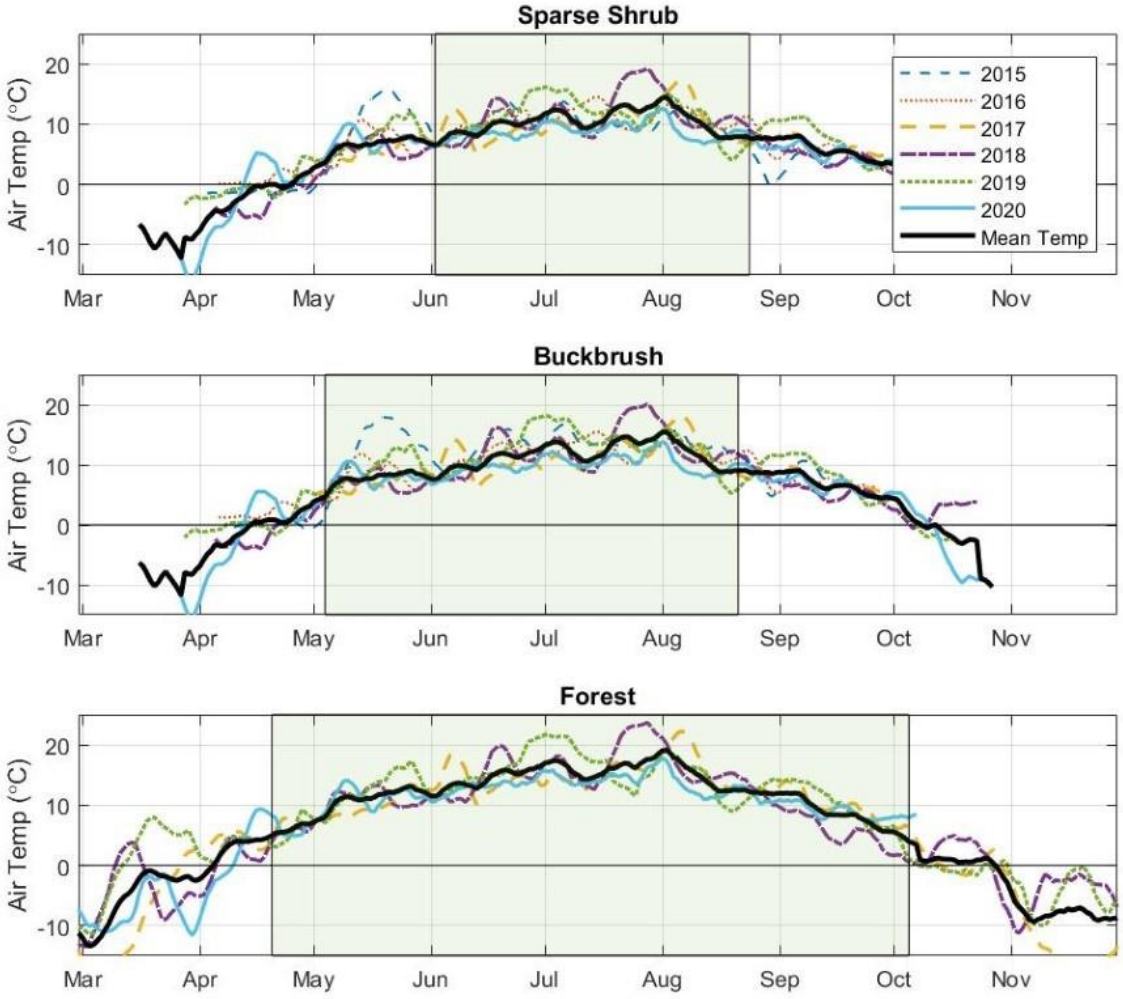

Figure 2. 7-day moving mean daily temperatures for Forest (top), Buckbrush (middle) and Sparse Shrub (bottom) for all available years of data. Shaded green regions show mean growing season. The start of the growing season was defined as the first of at least three consecutive days with net ecosystem exchange (NEE) less than 0 g C m^{-2} and the end of the growing season was defined as the first day where NEE was greater than 0 g C m^{-2}.

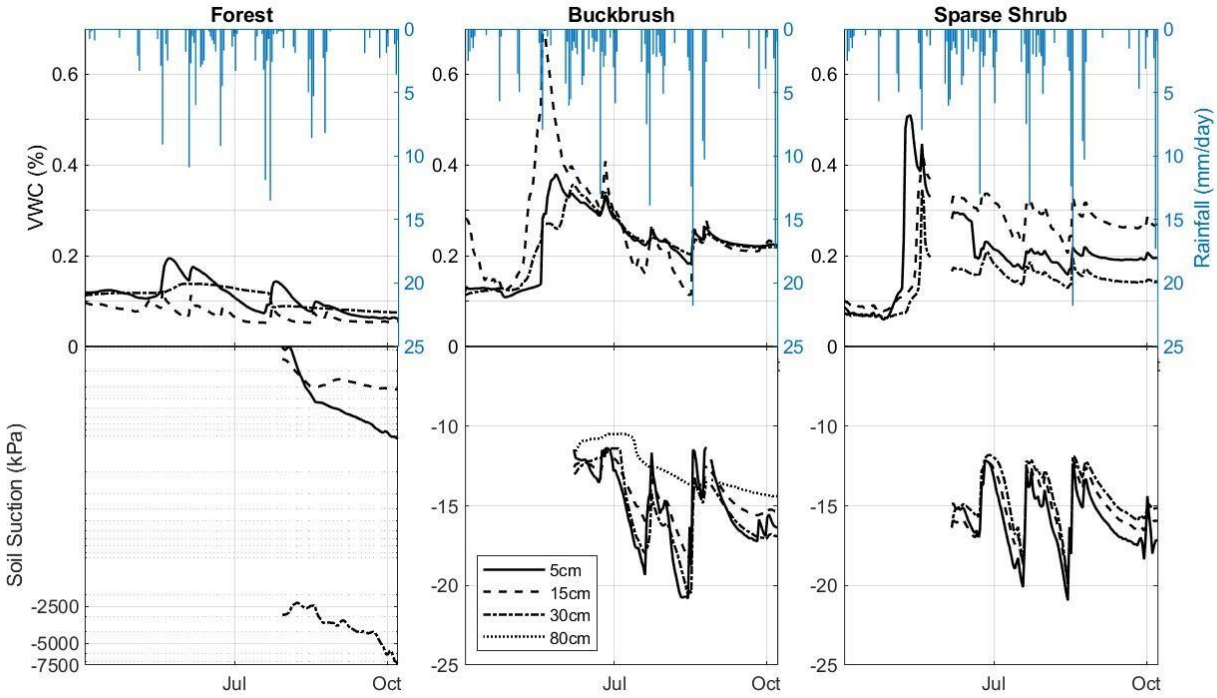

Figure 3. Half-hour volumetric water content (VWC) and daily rainfall (top) and half-hour soil tension (bottom) at Forest (left), Buckbrush (middle), and Sparse Shrub (right) in 2019.

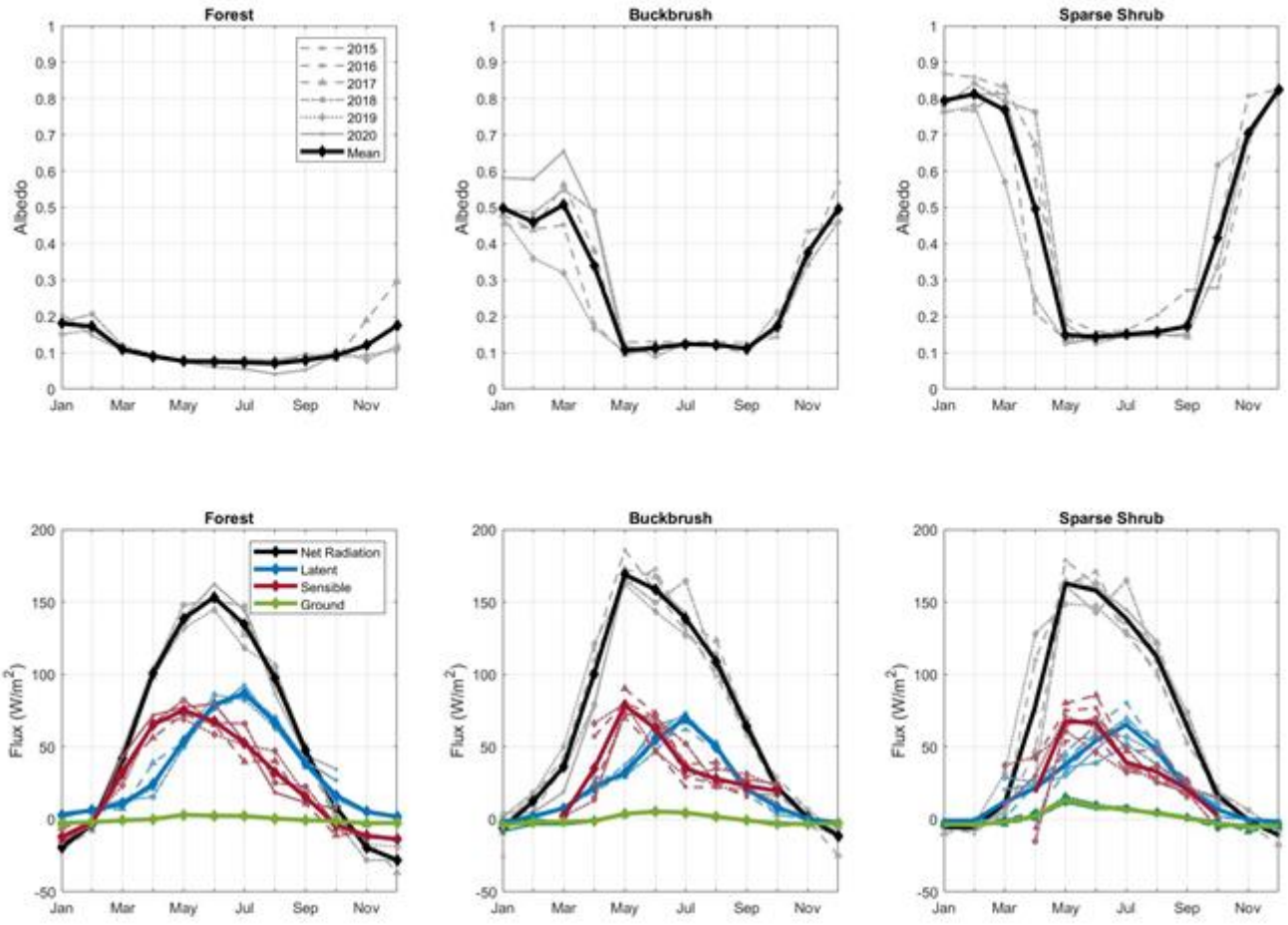

Figure 4. Monthly mean mid-day (11:00-14:00) albedo for Forest (left), Buckbrush (middle), and Sparse Shrub (right) for 2015-2020 (top) and monthly mean surface energy budget terms (Net Radiation (R_n), Latent heat ($\lambda_v E$), Sensible heat (H), Ground Heat Flux (G) for Forest (left), Buckbrush (middle), and Sparse Shrub (right) from 2015 to 2019 (bottom).

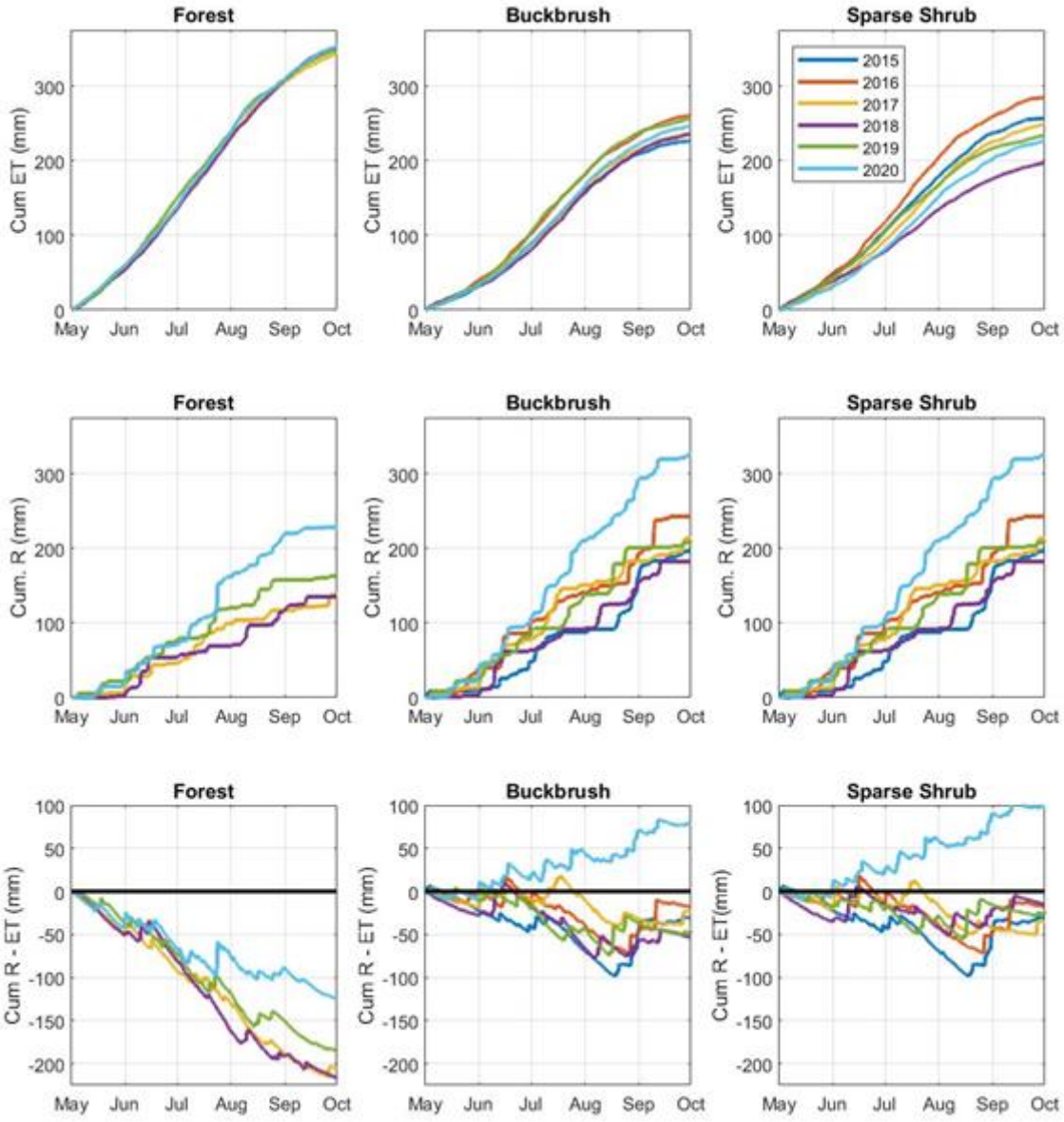

Figure 5. Cumulative gap-filled May to September ET (top) and cumulative daily rainfall (bottom) at Forest (left), Buckbrush (middle), and Sparse Shrub (right) from 2015-2020.

620

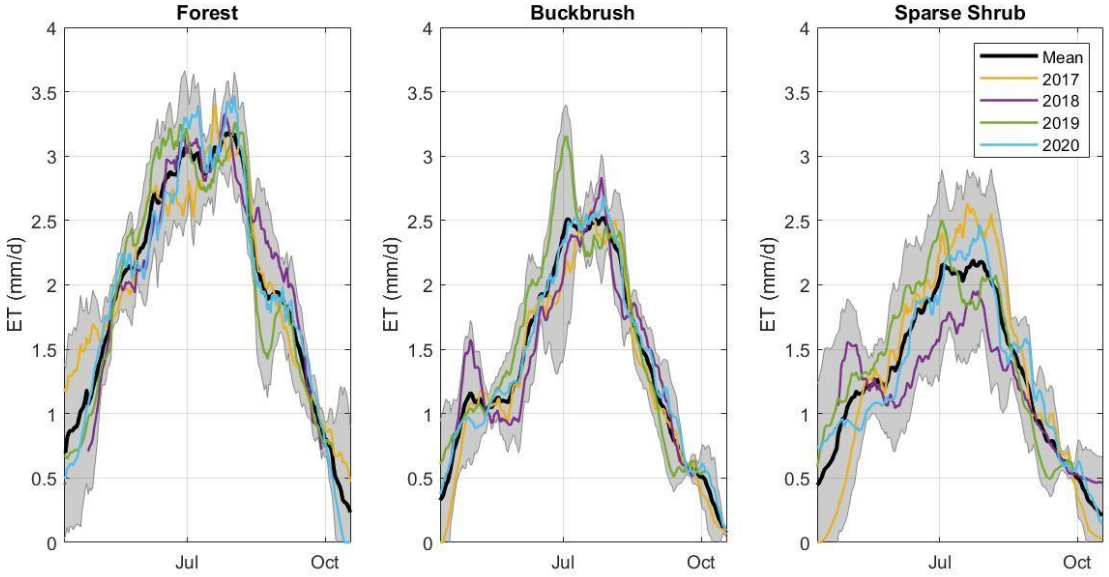

Figure 6. Moving 14-day daily ET rates at Forest (left), Buckbrush (middle), and Sparse Shrub (right) from 2017 to 2020 and the overall mean during these years. Two standard deviations from the mean are shown in shaded grey.

625

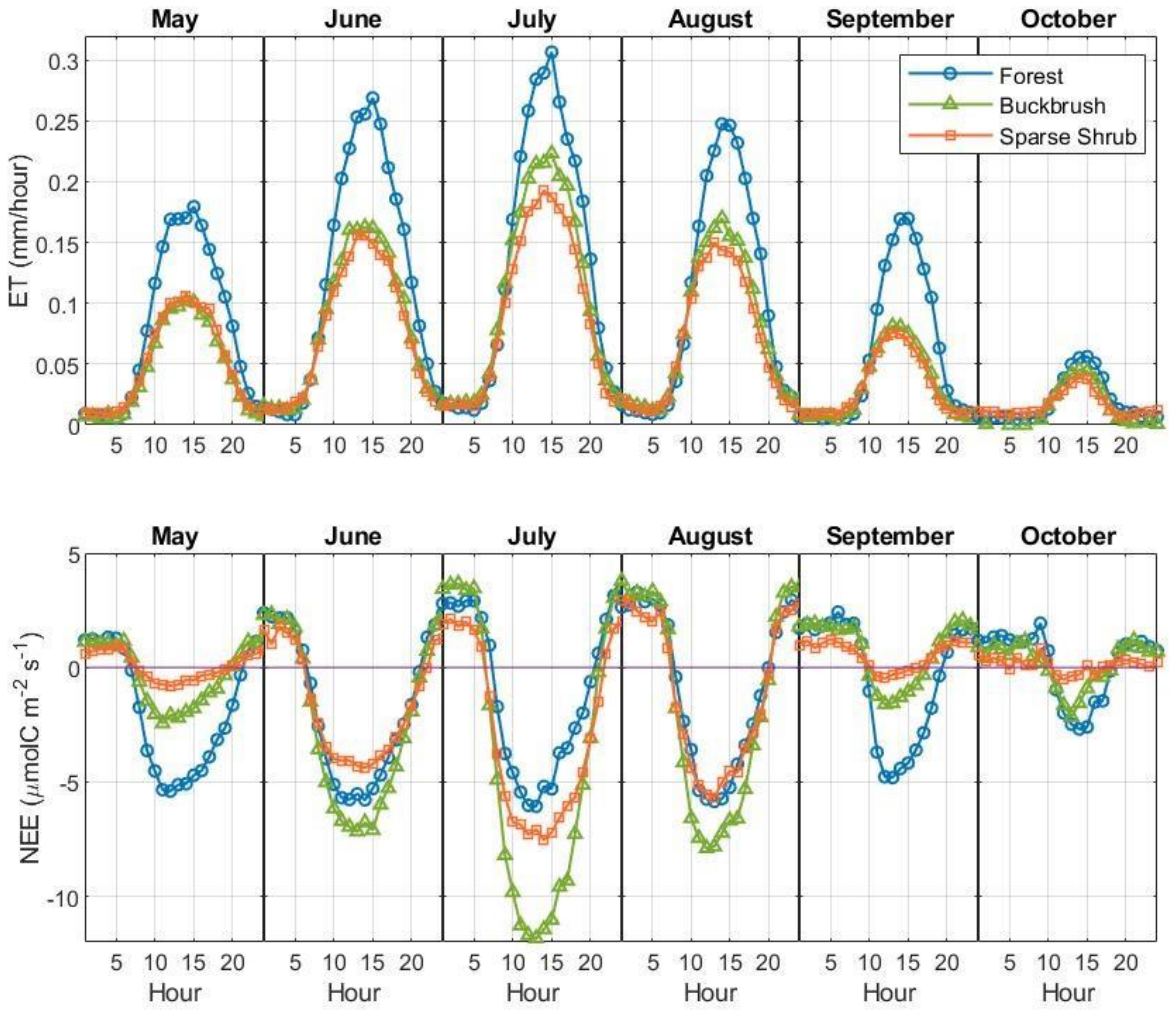

Figure 7. Mean monthly diurnal ET rates and net ecosystem exchange (NEE) from 2017-2020 at Forest (left), Buckbrush (middle) and Sparse Shrub (right).

630

635

Tables

640

Table 1: Site and stand characteristics. (± Standard Deviation)

Site	Elevation (masl)	Mean LAI (m^2/m^2)	Primary Vegetation Cover	Tree /Stem Density (trees m^{-2} or stems m^{-2})	Height (m)
Forest	743	3.5	White Spruce (*Picea glauca*)	0.3	14.1 (±0.34)
Buckbrush	1250	2.5	Dwarf Birch (*Betula*)	23	0.83 (±0.45)
			Willow Shrub (*Salix*)	2	1.34 (±0.33)
Sparse Shrub	1425	1.7	Dwarf Birch (*Betula*)	44	0.41 (±0.16)
			Willow Shrub (*Salix*)	7	0.55 (±0.30)

645

650

655

660

665

Table 2. Mean May to September daytime (7:00:21:00) values of energy balance partitioning ($\lambda_v E$ /Rn,H/Rn, H/Rn, Bowen ratio (β)), VPD (kPa). Ta (°C) is average daily air temperature over the entire day. Rainfall (mm), ET (mm), and ET:R represent totals over this period.

Site	Year	$\lambda_v E$ /R_n	H/R_n	G/R_n	β	VPD (Pa)	T_a (°C)	Rainfall (mm)	ET (mm)	ET:R
Forest	2017	0.47	0.43	0.01	0.92	452	11.1	138	344	2.50
	2018	0.46	0.45	0.01	0.97	559	10.9	135	352	2.60
	2019	0.48	0.47	0.01	0.97	651	12.0	165	347	2.11
	2020	0.49	0.45	0.01	0.91	484	10.3	228	353	1.55
	Average	0.47	0.45	0.01	0.94	536	11.1	166	349	2.19
	STD	0.01	0.01	0.00	0.02	69	0.6	34	3	0.37
Buckbrush	2015	0.28	0.32	NA	1.16	677	8.2	196	257	1.31
	2016	0.33	0.41	0.03	1.23	705	8.5	243	261	1.07
	2017	0.29	0.40	0.02	1.40	475	7.8	213	238	1.11
	2018	0.32	0.49	0.02	1.55	594	8.1	182	236	1.29
	2019	0.33	0.43	0.03	1.28	579	9.2	211	257	1.22
	2020	0.32	0.41	0.03	1.30	440	7.2	325	246	1.17
	Average	0.31	0.41	0.01	1.32	578	8.2	209	249	1.20
	STD	0.02	0.05	0.00	0.13	96	0.6	47	10	0.09
Sparse Shrub	2015	0.31	0.34	0.06	1.09	435	7.1	196	234	1.19
	2016	0.39	0.43	0.07	1.11	479	7.6	243	285	1.17
	2017	0.32	0.45	0.07	1.42	438	6.9	213	249	1.17
	2018	0.27	0.46	0.06	1.73	558	7.2	182	197	1.08
	2019	0.31	0.40	0.07	1.29	505	8.2	211	234	1.11
	2020	0.29	0.41	0.07	0.91	489	6.4	325	227	1.08
	Average	0.31	0.41	0.07	1.34	484	7.2	209	240	1.14
	STD	0.04	0.04	0.00	0.26	42	0.6	47	26	0.05

Supplementary Material

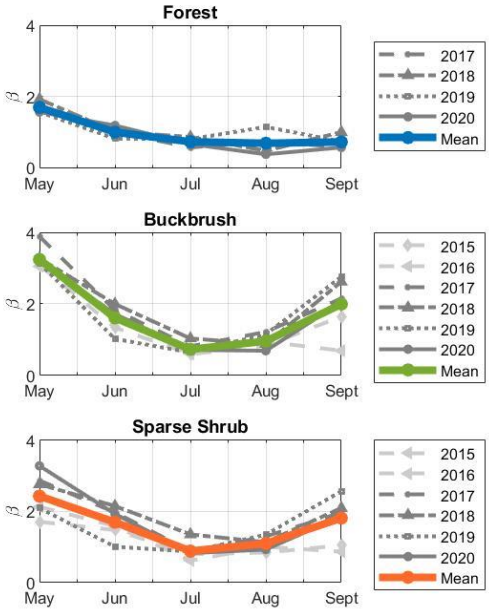

Figure S1. Monthly mean Bowen ratio (β) at Forest (top), Buckbrush (middle), and Sparse Shrub (bottom) in all years of available data.

685

690 **Table S1. Percent of missing data, energy balance closure, and R2 from artificial neural network (ANN) run to gap-fill missing data from 1 May to 30 September (DOY 121-273) at Forest, Buckbrush, Sparse Shrub.**

	Forest	Buckbrush	Sparse Shrub
Missing Data (May to Sept) (%)			
2015	NA	33	40
2016	NA	32	28
2017	34	32	29
2018	32	27	50
2019	51	23	63
2020	22	31	35
Mean	35	30	41
Energy Balance Closure (May to Sept)			
2015	NA	0.64	0.69
2016	NA	0.78	0.88
2017	0.85	0.76	0.94
2018	0.85	0.71	0.76
2019	0.85	0.76	0.79
2020	0.87	0.80	0.76
Mean	0.86	0.74	0.80
R^2 from Best ANN Run to Gap-Fill Latent Heat Data			
2015	NA	0.75	0.65
2016	NA	0.80	0.82
2017	0.81	0.77	0.79
2018	0.83	0.77	0.77

2019	0.84	0.75	0.72
2020	0.81	0.70	0.71
Mean	0.82	0.76	0.76
R^2 from Best ANN Run to Gap-Fill Sensible Heat Data			
2015	NA	0.94	0.94
2016	NA	0.95	0.95
2017	0.91	0.96	0.96
2018	0.92	0.88	0.89
2019	0.91	0.94	0.87
2020	0.90	0.84	0.86
Mean	0.91	0.92	0.91